


paper 9

 [CompositeStructures247\(2020\)112442](https://doi.org/10.1016/j.compstructs.2020.112442)

Contents lists available at [ScienceDirect](https://www.sciencedirect.com)

Composite Structures

journal homepage: www.elsevier.com/locate/compstruct

 Mechanical behavior of additively manufactured nanoclay/HDPE nanocomposites Pavan Beesettya, Aditya kalea, Balu Patilb, Mrityunjay Doddamanian^{a,*}

^a Advanced Manufacturing Lab, Mechanical Engineering, National Institute of Technology, Karnataka, Surathkal, India ^b Enerzi Microwave Systems Pvt. Ltd., Belgaum, India

ARTICLE INFO

Keywords: Nanoclay HDPE

Nanocomposite Filament

3D printing

ABSTRACT

Nanoclay (NC) has blended with relatively inexpensive, widely consumed HDPE (high density polyethylene) for the development of filament to be used in 3D printers [Code a1]. NC/HDPE blends are prepared by varying NC wt. % (0.5, 1, 2, and 5) and are subjected to meltflow index (MFI) measurements [Code a3]. MFI has noted to be decreasing with NC loadings. [Code a4] NC/HDPE nanocomposite blends are further extruded using a single screw extruder. [Code a3] Developed nanocomposites filaments are fed to the fused filament fabrication (FFF) based 3D printer for realizing NC/HDPE nanocomposite prints. [Code a3] The density of printed sample increases with filler content [Code a4]. Filament and printed samples thermal study is carried out using differential scanning calorimeter (DSC) [Code a3]. NC addition increases crystallinity and crystallization temperature without significant change in melting peak temperature. [Code a4] Freeze fractured prints reveal the uniform distribution of NC in HDPE. [Code a4] The tensile test is conducted on the filaments and prints. Further printed nanocomposites are subjected to flexural investigations [Code a3]. Tensile modulus and strength of filament increase with NC additions in HDPE matrix. [Code a4] Tensile and flexural properties (modulus and strength) of the nanocomposite prints increases with NC content. [Code a4] Finally, results obtained from the tensile and flexural tests of prints are compared with different HDPE composites available in the literature. [Code a5]

1. Introduction

Among the polymer based additive manufacturing (AM) techniques, FFF is the most commonly used, widely exploited approach in developing custom made geometrically complex components. AM researchers, academicians, and industrial practitioners use FFF based AM to rapidly develop tangible objects and functional parts. It allows user to manufacture highly complex parts very easily as compared to conventional manufacturing processes [1–3]. In the FFF process, the thermoplastic based filament is passed to

liquefier of 3D printer through the electromechanical drive. In the liquefier, plastic gets converted into semi-molten state. The extrusion head of the printer, layer it down as per part geometry defined by the STL file [4]. Limited options of commercial filaments limit the exploitation of the FFF process to manufacture the complex functional products. The newly developed filament must have certain mechanical properties and should be compatible with existing machines without modifying its software/hardware components [5–7]. Till date, commonly used filament materials include but not limited to, polyetherimide, acrylonitrile butadiene styrene [8], polylactide [9], polymethylmethacrylate [10], polycarbonate [11] and their blends [12,13], polycaprolactone [14],

polybutylene terephthalate [15], polyamide [16], polypropylene [17,18] and HDPE[19,20]. Major issues associated with printing with thermoplastic material includes layer delamination and part shrinkage/ warpage as a result of repetitive heating and cooling cycles[21,22]. 3D printed composite parts printed by FFF have superior properties compared to their neat counterparts[23]. The FFF method has been commonly preferred in various sectors such as medical [24,25,87], automotive[26], and aeronautics[27]. In such scenarios, need for widening the scope of newerfilaments developments is crucial and is the focus of present work. Recently researchers are taking up intensive developmental works to explore and enhancefilaments material properties by combining a wide range of fillers with thermoplastics using compounding techniques. Fillers such as iron particles [28], carbon and glass fiber [29], Al_2O_3 powder [30], glass microspheres [31], and fly ash cenospheres [32,33] are being used in the literature to enhance thermoplastic filaments mechanical behavior. Present work is focused on increasing filament material choices for the FFF technique by developing nanocomposite feedstock.

In recent years, the composite community widely explored organically modified nanoclay like montmorillonite (MMT) by reinforcing it in polymers [34–37]. The ability of tailoring the different properties by

* Corresponding author.

E-mail address: mraddamani@nitk.edu.in (M. Doddamani).

<https://doi.org/10.1016/j.compstruct.2020.112442>

Received 13 April 2020; Received in revised form 28 April 2020; Accepted 29 April 2020

Available online 04 May 2020

0263-8223/©2020 Elsevier Ltd. All rights reserved.

Nomenclature

ρ_{th} Theoretical density (kg/m^3)

ρ_{exp}

Experimental density (kg/m^3)

ρ_C Composite density (kg/m^3) ρ_H HDPE density (kg/m^3) ρ_{NC} NC density (kg/m^3) w_H HDPE (wt. %) w_{NC} NC (wt. %)

T_{Melt} Peak melting temperature ($^{\circ}\text{C}$) T_{Cryst} Crystallization temperature ($^{\circ}\text{C}$)

α_{Cryst} Degree of crystallinity (%) Flnt Filament

Prnt 3D Print

combining various matrix and filler widens the application domain of nanocomposites. Strong molecular interaction between polymer resin and nanofiller improves the thermal, mechanical, and physical properties of nanocomposites [38]. Polymer nanocomposites find their application in various sectors such as automotive (body interior, under-the-hood, and exterior), electrical and electronics industries (electric components and

printed circuits), construction (shaped extrusions, panels, etc.), food packaging (films, containers), filling materials in dentistry, cosmetics, beverage and food packaging, biomedical applications, military, and aerospace [39]. Clay based nanocomposites are specifically utilized in fire retardancy applications [40]. NC has ideally used reinforcement among the available nanoparticles due to lower cost, easy availability, higher cation exchange capacity and aspect ratio. It can be surface treated as well with various surfactants for enhancing mechanical properties [41]. HDPE is widely used industrial thermoplastic polymer because of its more distinct physical and mechanical properties compared to other thermoplastics [42]. HDPE find its applications in milk jugs, household utilitarian products, packaging industries and in many structural applications [43,44]. Some of the commonly used fillers with HDPE are carbon nanotubes [45], fly ash cenospheres [46–48], glass microballoons [49–51], carbon [52], calcium carbonate [53], graphite nanofibers [54], etc. Compared to conventional macro/micro filler reinforced composites, NC, in small quantities (≤ 5 wt. %) exhibits significant improvement in mechanical properties [55].

Commonly used polymers with nanoclay are polyethylene [56], polypropylene [57–59], polyethylene terephthalate [60], polystyrene [61,62] and polyamide [63]. HDPE is yet to be explored with NC for realizing complex geometrical components through 3D printing. Excellent biocompatibility and mechanical properties of HDPE can be exploited further by reinforcing it with NC. Such an NC inclusion might effectively reduce the warpage/shrinkage related issues in 3D printing [19,64]. Present work focusses on the development of NC/HDPE blends, filaments and prints. Blends are investigated for MFI first. The compounded blend of nanocomposite is used to extrude feedstock filament. Prior to printing, filaments are investigated for α_{Cryst} and tensile behavior.

Subsequently these nanocomposite filaments are used as feedstock inputs in FFF based 3D printer. Further, 3D printed nanocomposites are investigated for crystallinity, tensile and flexural responses. Finally present work is compared with other HDPE composites in the property map.

1. Experimental

2.1. Materials, blend preparation and MFI measurements

HDPE (HD50MA180) granules used in the present study are supplied by Reliance Polymers, Mumbai. Table 1 provides property details of HDPE resin [6]. Montmorillonite K 10 powder (NC) is procured from SIGMA-ALDRICH, India. It is offwhite in appearance, having a density of 1980 kg/m^3 . Compounding of HDPE and NC (0.5, 1, 2, and 5 wt. %) in as received conditions (without any surface treatment) is materialized using 16CME SPL Brabender at 210°C [65] to get the nanocomposite pellets (Fig. 1a). Blends with 0.5, 1, 2, and 5 wt. % NC in neat HDPE (H) are designated as H0.5, H1, H2, and H5, respectively. Dy-

estimations (ASTM D1238-13) of NC/HDPE nanocomposite blends. MFI provides basic knowledge of material flow with respect to the unit time and viscosity change due to nanoparticle addition, which in turn helps to set optimum printing parameters in the commercially available 3D printers.

2.2. Filament development and 3D printing

NC/HDPE pellets obtained from Brabender (Fig. 1a) are fed into the single screw extruder to extrude nanocomposite filament (Fig. 1b). The single screw extruder and 3D printer being used in this study are respectively from Asabi Machinery Pvt. Ltd., Mumbai (L/D ratio –25:1, 25SS/MF/26) and Star, AHA 3D Innovations, Jaipur. The extruder has three heating zones with a temperature setting of 160, 165, and 150°C , respectively. Feed section temperature is maintained constant at 155°C . These parameters are optimized based on the uniform and consistent flow through the die [6]. Take-up unit and screw rotation are set as 12.5 and 25 rpm respectively to extrude the H–H5 filaments with a consistent diameter of $2.85 \pm 0.05 \text{ mm}$

(Fig. 1b). Fig. 1b shows an image of a representative H5 filament having consistent diameter without any surface irregularities/defects. A similar setting is maintained for extruding other compositions as well. Extruded NC/HDPE filaments are fed to a commercially available 3D printer. Table 2 provides details of optimized printing parameters based on uniform flow through the nozzles, defect-free deposition (inter and intra-layer), and warpage-free samples [6]. Printing speed is maintained at 100 mm/s, which is 3.7 times higher compared to our earlier works reported in Ref. [6]. Higher print speed is chosen by keeping industrial requirements in focus amid compromising mechanical properties of neat HDPE in particular as compared to reported investigations [6]. Infill is kept at 100% for comparative analysis with other dense HDPE composites.

2.3. Density measurement

Printed nanocomposites density is experimentally measured as per the ASTM D792-13 standard, and the average values are reported in Table 3. Theoretical densities of all the compositions are computed based on individual constituent materials density using, 1

$$\rho =$$

$$c w_H w_{NC}$$

$$+$$

$$\rho_H \rho_{NC} \quad (1)$$

Densities of HDPE and NC are taken as 950 and 1980 kg/m³ respectively.

Table 1

Typical characteristics of HDPE granules [6].

Property Typical value

MFI (190 °C/2.16 kg) 20 gm/10 min.

Density (23 °C) 950 kg/m³

Tensile strength at yield 22 MPa

Elongation at yield 12 %

Flexural modulus 750 MPa

Vicat softening point 124 °C

nisco LMI5000 laboratory melt flow indexer is utilized for MFI



Fig. 1. Representative (a) NC/HDPE blend and (b) H5 nanocomposite filament.

Table 2

Printer setting and parameters selected in the present work [6].

Printing parameters Typical value Nozzle temperature (°C) 250

Printing bed temperature (°C) 70

Layer thickness (mm) 0.35

Printing speed (mm/sec) 100a

Printing pattern Rectilinear

Part orientation Y-axis

Infill (%) 100

^a Set for higher productivity.

2.4. Differential scanning calorimetry of feedstock filament and their prints

DSC analysis of the filaments and prints is carried out using Perkin Elmer DSC-6000, USA with the cycles a) 0–200 °C heating and 3 min hold at 200 °C b) 200 –0 °C cooling and holding at 0 °C for 3 min., and c) second heating cycle from 0 to 200 °C. Approximately 10 mg of sample mass in 30 µl Al crucible is used. 10 °C/min heating and cooling rate is maintained constant throughout the test. Thermal stresses embedded in the previous processing step are removed using the first heating cycle. T_{Cryst} and T_{Melt} are estimated from cooling and heating cycles. DSC curves typically comprise exothermic and endothermic peaks and cold crystallization melting enthalpy peak. α_{Cryst} is computed from melting enthalpy values using,

2.5.

Tensile and flexural characterization

Tensile property characterization of the filament and 3D prints is carried out through Zwick Roell (Z020, load cell: 20 kN) UTM at 5 mm/ min as per the procedure outlined in ASTM D638-14. Extensometer (2— inch gauge length) is utilized for measurements with an initial load of 0.1 MPa. Flexural test (1.54 mm/min displacement rate, pre load of 0.1 MPa) is conducted on prints based on the D790-17 ASTM standard. Moduli in

flexure (E_f) is computed using, $E = \frac{L^3 m}{4bd^3}$ (L: span length, m: slope, b: width, d: thickness) (3) Flexural stress (ρ_{fm}) is estimated using, $\rho_{fm} = \frac{3PL}{2bd^2}$ (P – load)

1. Results and discussion

3.1. MFI

MFI of NC/HDPE nanocomposites representing the flowability characteristic is presented in Fig. 2a. It is well-known fact that, the variation in MFI is inversely proportional to the change in melt viscosity. NC particles resist the polymer chain mobility and reflect into the

$$\alpha_{Cryst} = \frac{\Delta H_m}{\Delta H^*} \times 100$$

$$\Delta H^*$$

$$m$$

$$(2)$$

lower MFI values in nanocomposites [67]. With increasing NC content in the HDPE matrix, MFI decreases, which accounts for 18.04, 17.14, 15.29, and 13.97 gm/10 min, respectively, for H0.5–H5. Pristine HDPE

where, ΔH_m is heat of fusion (J/g) and ΔH^*

$$m$$

crystalline HDPE/gram (293 J/g [66]).

is the fusion heat for registered MFI of 23.06 gm/10 min [6]. MFI decreases in the range of 21.77–39.42 % for H0.5–H5 nanocomposites, respectively, as compared H. A similar trend is observed in Ref.[67,68]. As MFI reductions in the developed nanocomposite blends are less than 60%, a multiplier is set at ‘1’ in the commercially available printer for all the compositions.

Table 3

ρ_{th} , ρ_{exp} , T_{Cryst} , α_{Cryst} and T_{Melt} estimations of samples.

Material	Prnt.		T_{Cryst}		α_{Cryst}		T_{Melt}	
	ρ_{th}	ρ_{exp}	Flnt	Prnt	Flnt	Prnt	Flnt	Prnt
H	950.00	948.93 ± 13	108.02	109.05	55.5	57.1	131.07	131.02
H0.5	952.48	998.30 ± 16	111.44	111.77	56.7	72.9	131.66	130.90
H1	954.97	998.60 ± 26	112.32	112.67	57.1	73.8	131.03	131.67
H2	959.99	999.20 ± 11	112.64	112.74	65.8	75.3	131.24	130.29
H5	975.37	999.40 ± 18	112.05	112.40	68.0	77.8	131.26	130.62



Fig. 2. (a) MFI of NC/HDPE nanocomposites and (b) Micrograph of a representative freeze fractured H2 print.



Fig. 3. DSC curves for filaments (a), (b) and prints (c), (d).

3.2. Density and DSC investigations

The densities of prepared filaments and prints are presented in Table 3. The addition of hard and stiff NC into HDPE increases the composite density. Among all the compositions, H5 has shown the highest density as expected. Higher experimental densities, as compared to the respective theoretical ones except H, clearly indicate dense prints and absence of matrix porosity. Uniform distribution of hard and stiff NC particles into HDPE is clearly observed through SEM of representative 3D printed sample (Fig. 2b). Interfacial bonding between NC and HDPE is observed to be poor as constituents materials utilized in the present work are not surface treated. DSC results of filaments and prints are presented in Table 3. Fig. 3 presents the DSC curves of the filament and printed HDPE and their nanocomposites. Compared to HDPE all the filament and 3D printed samples have shown higher T_{Cryst} temperature indicating strong interaction between HDPE resin and

Table 4

Tensile test result of filament and 3D prints.

Material Modulus (MPa) UTS (MPa) Elongation at UTS (%) Fracture strength (MPa) Fracture strain (%)

	Flnt	Prnt	Flnt	Prnt	Flnt	Prnt	Flnt	Prnt	Flnt	Prnt
H	525 ± 11	874 ± 12	11.1 ± 0.1	13.8 ± 0.2	11.4 ± 0.2	13.0 ± 0.2	—	6.0 ± 0.19	—	160.1 ± 3.3
H0.5	677 ± 15	904 ± 13	13.8 ± 0.3	15.0 ± 0.3	12.6 ± 0.4	12.1 ± 0.2	9.8 ± 0.12	14.1 ± 0.22	26.1 ± 0.6	19.0 ± 0.6
H1	683 ± 16	914 ± 17	13.9 ± 0.3	15.1 ± 0.4	11.8 ± 0.2	11.0 ± 0.4	2.30 ± 0.08	13.9 ± 0.54	51.9 ± 1.1	19.6 ± 0.3
H2	710 ± 20	946 ± 22	14.3 ± 0.5	15.6 ± 0.3	11.4 ± 0.4	8.8 ± 0.3	1.57 ± 0.05	12.0 ± 0.47	63.5 ± 2.1	19.6 ± 0.6
H5	741 ± 21	949 ± 20	14.9 ± 0.2	16.9 ± 0.1	11.4 ± 0.3	8.1 ± 0.1	1.49 ± 0.05	9.0 ± 0.29	69.2 ± 1.2	9.0 ± 0.33



Fig. 4. Representative (a) tensile stress–strain plots of neat H–H5 (b) micrograph of H5 and (c) H2 filaments.

nanoclay particles. During cooling cycle of H, at significantly higher temperature, the melt nucleates on the NC surface leading to the formation of larger thickness crystal lamellas resulting in higher T_{Cryst} [69,70]. 3D prints and filament shows similar T_{Cryst} trend which indicates that the

second material extrusion through printers nozzle has no remarkable impact. No significant difference is observed in T_{Melt} of the filament and prints (Table 3). Polymer chains have a tendency to crystallize by their own (self-nucleation effect) or due to external nucleating agents. In the present nanocomposite filaments and prints, NC has played the role of external nucleating agent enhancing crystallization. The higher percentage of crystallization in 3D prints as against respective filaments is attributed to more aligned material extrusion and natural cooling of the prints in the printer chamber [71]. Prints cool down by natural convective mode, whereas hot extruded filament is being quenched in a water bath during filament extrusion. Thus the polymer melt has less time to crystallize, enabling the chains to align in random order. Degree of crystallinity increases as nanoclay concentration increases in filaments and prints. α_{Cryst} increased from 57.1%

to 77.8% for H–H5, respectively, in prints. Higher α_{Cryst} in 3D printed samples as against respective nanocomposite filaments is attributed to the different cooling modes in the respective processing routes [72].

3.3. Tensile testing of filaments and prints

The filament should have sufficient strength and stiffness to be used as feedstock in commercially available 3D printers. It should not rupture or buckle while passing through a filament drive mechanism [73]. Filament buckling can be avoided by making it stiff enough such that it will pass through the drive mechanism successfully. Inclusion of NC improves the stiffness of nanocomposite filament. Modulus of nanocomposite filament has increased with NC addition. Among the nanocomposite filament, H5 has registered the highest modulus 741 MPa (Table 4) and is 41.14% higher compared to H. Filament stiffness is improved by stiff and hard NC additions in compliant HDPE resin. Stress–strain plots for HDPE and the composite filament is plotted in Fig. 4a until 15% strain as neat HDPE filament exhibits more than 150% strain level. The test is stopped

due to stroke distance and time constraints. Such a higher strain value signifies the ductile behavior of neat



Fig. 5. Representative (a) stress–strain curve for 3D prints and freeze fractured micrographs of (a) H and (b) H5 prints post tensile test.

Table 5

Specific tensile properties of printed H–H5.

Material	Sp. Modulus (MPa/kg/m ³)	Sp. Strength (MPa/kg/m ³) × 10 ⁻³
----------	--------------------------------------	--

HDPE.	On the contrary, nanocomposite filament elongation decreased severely. The tensile strength of H5 (14.90 MPa) is highest among all the composition, which is ~35% higher compared to neat HDPE filament. Uniform distribution of NC in H for H5 (Fig. 4b) compared H2
-------	---

(Fig. 4c) might be the reason for such an observation. Further, there may be better molecular level interface inconsonance occurring between the polymer chain and nanoclay at H5. Elongation at UTS is highest for H0.5 in filaments. The fracture strength and strain of nanocomposite filaments are significantly lower compared H, which might be due to a reduction in HDPE deformation post-NC additions.

H	0.921	14.58
---	-------	-------

H0.5	0.906	15.03
------	-------	-------

H1 0.916 15.12

H2 0.947 15.61

H5 0.950 16.91

The tensile behavior of printed H–H5 is presented in Fig. 5, and the values are presented in Table 4. Printed samples failed typically in 

Fig. 6. Representative (a) flexural stress–strain plot for 3D prints and (b) SEM of H5 post flexural test.

Table 6

Flexural properties of prints.

Material	Modulus (MPa)	Strength (MPa)	Specific modulus (MPa/kg/m ³)	Specific strength (MPa/kg/m ³)× 10 ^{−3}
H	656 ± 13	19.90 ± 0.06	0.69	20.97
H0.5	662 ± 12	20.20 ± 0.04	0.66	20.23
H1	672 ± 13	20.80 ± 0.02	0.67	20.83

H2	697 ± 16	21.50 ± 0.03	0.70	21.52
H5	735 ± 13	22.24 ± 0.03	0.74	22.25



Fig. 7. (a) Tensile modulus and (b) strength of HDPE composites. Fig. 8. (a) Flexural modulus and (b) strength of HDPE composites.

brittle mode except for neat HDPE. Printed H exhibited ~160% fracture strain though plots in Fig. 5a are graphed until 18% strain. Fig. 5b shows a micrograph of H, which clearly indicates substantial plastic deformation of the HDPE matrix. Nanocomposites modulus increases as filler loading rises (Table 4). H5 composition has shown maximum modulus across all the NC variations and is 8.58% higher relative to H.

3D printed H–H5 modulus is 1.66, 1.34, 1.34, 1.33, and 1.28 times higher than their respective filament which is attributed to the polymer chains realignment and augmented crosslinking in printing. H5 exhibited the highest UTS of 16.9 MPa, which is 22.46% higher as compared to H. Higher surface area rendered by NC might be the reason for effective load transfer between the constituents leading to such an observation. UTS of prints registered better responses compared to their respective filaments. Elongation at UTS decreases with increasing NC content due to the reduction of compliant HDPE content with higher filler loadings. Fracture strength of H5 print is higher by 50% compared to H, while the fracture strain of H5 is substantially lower compared to neat HDPE. Specific mechanical properties are crucial from a structural application perspective. Specific strength of H5 outperformed H by 16% (Table 5).

3.4. Flexural response of prints

Neat HDPE and their nanocomposite prints did not fail until 10% strain (Fig. 6a). Flexural moduli and strength of nanocomposite increase with NC loading (Table 6). The restrictions posed by NC particles effectively hinders the matrix flow. The higher surface area of nanoscale reinforcements might bind the polymer chains together, resulting in the mechanical properties enhancements. Fig. 6b shows H5 micrograph post flexural tests. NC is firmly embedded in the matrix without any signs of locational shifts. This might be due to the enhanced mechanical interlocking between nanoscale NC and polymer chains owing to higher surface area offered by nanoscale reinforcements. Highest flexural modulus and strength are exhibited by H5,

which is 1.12 times respective values of H. H5 registered 1.07 and 1.06 times higher specific modulus and strength respectively compared to their neat counterparts.

Developed NC/HDPE nanocomposite prints reveal superior tensile and flexural properties compared to neat HDPE counterparts. These nanocomposite prints, especially H5, can be a potential candidate material in replacing a few geometrically complex injection and compression molded components. Further, NC addition reduces HDPE consumption to some extent. Nanocomposite filament development and its feasibility in 3D printing, as presented in this work, also widens feedstock filament choices availability for polymer-based additive manufacturing community.

1. Property chart

Tensile and flexural properties are plotted against the density of HDPE composites for different types of filler in Fig. 7 [6,46,74–81] and Fig. 8 [74–76,79,82–86] respectively based on the data extraction from published literature for comparative analysis. It is clearly depicted by these plots, that the solid particle reinforced composites have higher density and modulus as expected. However, printed NC/HDPE nanocomposite exhibits higher density, lower modulus, and higher strength compared to 3D printed fly ash based composites (Fig. 7). Tensile modulus of nanocomposite print is better as compared to lignocellulose, carbon black, wood, cenospheres, CaCO_3 , and glass microsphere-based HDPE composites (Fig. 7a). Tensile strength is higher compared to 3D printed, injection and compression molded HDPE base system (Fig. 7b). The flexural moduli of the nanocomposites are lower as compared to 3D printed, injection and compression molded foam system (Fig. 8a). Printed nanocomposites strength in flexure is higher against wood powder—filled and natural fiber composites, and less compared to compression molded samples as seen from Fig. 8b. Nonetheless, these nanocomposites registered superior performance as compared to 3D printed and injection molded fly ash based foams. This property chart reveals the potential usage of NC in the HDPE matrix that can be exploited over a wide range of mechanical properties for different functional components.

1. Conclusions

NC/HDPE nanocomposite feedstock filaments feasibility is successfully demonstrated for commercially available 3D printers. Developed filaments and 3D prints are studied for their thermal and mechanical properties. Observations are listed below as:

NC/HDPE nanocomposites are successfully printed without any warpage.

-

- MFI of nanocomposite blends decrease with increasing NC content, whereas crystallinity is observed to be increasing. H–H5 filaments

crystallinity decreased as against respective prints.

-

Tensile and flexural, modulus and strength are noted to be increased with NC additions in compliant HDPE matrix.

-

H5 is the best composition exhibiting superior mechanical performance.

-

Property map reveals the suitability of NC/HDPE nanocomposite printing with enhanced mechanical properties as compared to other HDPE composites synthesized through conventional and advanced manufacturing technologies.

The aim of the present work is to materialize nanocomposite filaments for 3D printing applications to widen the scope of limited material choices available for the FFF based additive manufacturing community.

CRedit authorship contribution statement

Pavan Beesetty: Methodology, Investigation, Writing - original draft.
Aditya kale: Methodology, Investigation, Writing - original draft. Balu Patil: Methodology, Writing - review & editing. Mrityunjay Doddamani: Conceptualization, Writing - review & editing, Visualization, Supervision.

Declaration of Competing Interest

The authors declare that they have no known competing financial interests or personal relationships that could have appeared to influence the work reported in this paper.

Acknowledgment

Authors thank the Department of Mechanical Engineering at NITK for providing support and the research facilities. Mrityunjay Doddamani acknowledges the grant (VGST/GRD-606/133) by Vision Groupon Science and Technology, Dept. of Information Technology, Biotechnology and Science and Technology, Govt. of Karnataka.

Data availability

The raw/processed data required to reproduce these findings cannot be shared at this time as the data also forms part of an ongoing study.

References

- [1] [Doddamani M. Dynamic mechanical analysis of 3D printed eco-friendly lightweight composite. Compos Commun 2020;19:177–81.](#) [2] Gupta Nikhil, Doddamani Mrityunjay. 3D printing of syntactic foams for marine applications. In: Lee SW, editor. Advances in thick section composite and sandwich structures: an anthology of ONR-sponsored research Cham: Springer International Publishing; 2020. p. 407–38. https://doi.org/10.1007/978-3-030-31065-3_14.
- [3] [Patil B, Bharath Kumar BR, Doddamani M. Compressive behavior of fly ash based 3D printed syntactic foam composite. Mater Lett 2019;254:246–9.](#) [4] [Dakshinamurthy D, Gupta S. A Study on the influence of process parameters on the viscoelastic properties of ABS components](#)

[manufactured by FDM process. J Inst Eng \(India\) Ser C 2018;99:133. \[5\] Singh R, Singh S, Mankotia K. Development of ABS based wire as feedstock filament of FDM for industrial applications. Rapid Prototyp J 2016;22:300–10. \[6\] Patil B, Bharath Kumar BR, Bontha S, Balla VK, Powar S, Hemanth Kumar V, et al. Eco-friendly lightweight filament synthesis and mechanical characterization of additively manufactured closed cell foams. Compos Sci Technol 2019;183:107816. \[7\] Singh AK, Deptula AJ, Anawal R, Doddamani M, Gupta N. Additive manufacturing of three-phase syntactic foams containing glass microballoons and air pores. JOM 2019;71\(4\):1520–7. \[8\] Dul S, Pegoretti A. Fused deposition modeling with ABS-graphene nanocomposites.](#)

[Compos A Appl Sci Manuf 2016;85:181–91.](#)

[\[9\] Arivazhagan A, Saleem A, Masood S, Nikzad M, Jagadeesh K. Study of dynamic mechanical properties of fused deposition modelling processed ultem material. Am J Eng Appl Sci 2014;7:307–15. \[10\] Domingo-Espin M, Puigoriol-Forcada JM, Garcia-Granada A-A, Llumà J, Borros S,](#)

[Reyes G. Mechanical property characterization and simulation of fused deposition modeling polycarbonate parts. Mater Des 2015;83:670–7.](#)

[\[11\] Spoerk M, Arbeiter F, Cajner H, Sapkota J, Holzer C. Parametric optimization of intra— and inter-layer strengths in parts produced by extrusion-based additive manufacturing of poly\(lactic acid\). J Appl Polym Sci 2017;134:45401. \[12\] Espalin D, Arcaute K, Rodriguez D, Medina F, Posner M, Wicker R. Fused deposition modeling of patient-specific polymethylmethacrylate implants. Rapid Prototyp J 2010;16\(3\):164–73. \[13\] Wang X, Jiang M, Zhou Z, Gou J, Hui D. 3D printing of polymer matrix composites:](#)

[a review and prospective. Compos B Eng 2017;110:442–58.](#)

[\[14\] Stansbury JW, Idacavage MJ. 3D printing with polymers: challenges among ex- panding options and opportunities. Dent Mater Off Publ Acad Dent Mater 2016;32\(1\):54–64. \[15\] Xuan Y, Tang H, Wu B, Ding X, Lu Z, Li W, et al. A specific groove design for](#)

[individualized healing in a canine partial sternal defect model by a polycaprolactone/hydroxyapatite scaffold coated with bone marrow stromal cells. J Biomed Mater Res Part A 2014;102\(10\):3401–8.](#)

[16] [Tellis BC, Szivek JA, Bliss CL, Margolis DS, Vaidyanathan RK, Calvert P. Trabecular](#)

[scaffolds created using micro CT guided fused deposition modeling. Mater Sci Eng C Mater Biol Appl 2009;28\(1\):171–8.](#)

[17] [Silva M, Pereira AM, Alves N, Mateus A, Malça C. A hybrid processing approach to the manufacturing of polyamide reinforced parts with carbon fibers. Procedia](#)

[Manuf 2017;12:195–202.](#)

[18] [Carneiro O, Silva AF, Gomes R. Fused deposition modeling with polypropylene. Mater Des 2015;83:768–76.](#) [19] [Chatkunakasem P, Luangjuntawong P, Pongwisuthiruchte A, Aumnate C, Potiyaraj](#)

[P. Tuning of HDPE properties for 3D printing. Key Eng Mater 2018;773:67–71.](#)

[20] Gupta N, Zeltmann SE, Luong DD, Doddamani M. Testing of foams. In: Schmauder S, editor. Handbook of mechanics of materials Singapore: Springer Singapore; 2019. p. 2083–122. https://doi.org/10.1007/978-981-10-6884-3_50. [21] [Wang T-M, Xi J-T, Jin Y. A model research for prototype warp deformation in the](#)

[FDM process. Int J Adv Manuf Technol 2007;33:1087–96.](#)

[22] [Zhang Y, Chou K. A parametric study of part distortions in fused deposition modeling using three-dimensional finite element analysis. Proc Inst Mech Eng B J Eng Manuf 2008;222\(8\):959–68.](#) [23] [Kalsoom U, Nesterenko PN, Paull B. Recent developments in 3D printable composite materials. RSC Adv 2016;6\(65\):60355–71.](#)

[24] [Peltola SM, Melchels FPW, Grijpma DW, Kellomäki M. A review of rapid proto- typing techniques for tissue engineering purposes. Ann Med 2008;40\(4\):268–80.](#) [25] [Melgoza E, Vallicrosa G, Serenó L, Ciurana J, Rodriguez C. Rapid tooling using 3D](#)

[printing system for manufacturing of customized tracheal stent. Rapid Prototyp J 2014;20.](#)

[26] [Ilardo R, Williams C. Design and manufacture of a Formula SAE intake system using fused deposition modeling and fiber-reinforced composite materials. Rapid Prototyp J 2010;16:174–9.](#) [27] [Vashishtha V, Makade R, Mehla N. Advancement of rapid prototyping in aerospace industryda review. Int J Eng Sci Technol 2011;3.](#)

[28] Masood SH, Song WQ. Development of new metal/polymer materials for rapid tooling using Fused deposition modelling. Mater Des 2004;25(7):587–94. [https:// doi.org/10.1016/j.matdes.2004.02.009](https://doi.org/10.1016/j.matdes.2004.02.009). [29] [Brenken B, Barocio E, Favaloro A, Kunc V, Pipes B. Fused filament fabrication of](#)

[fiber-reinforced polymers: a review. Addit Manuf 2018;21.](#)

[30] [Singh R, Singh S, Fraternali F. Development of in-house composite wire based feed](#)

[stock filaments of fused deposition modelling for wear-resistant materials and structures. Compos B Eng \\$V 2016;98:244–9.](#)

[31] [Spoerk M, Arbeiter F, Raguž I, Weingrill G, Fischinger T, Traxler G, et al.](#)

[Polypropylene filled with glass spheres in extrusion-based additive manufacturing: effect of filler size and printing chamber temperature. Macromol Mater Eng 2018;303\(7\):1800179.](#)

[32] [Singh AK, Patil B, Hoffmann N, Saltonstall B, Doddamani M, Gupta N. Additive manufacturing of syntactic foams: Part 1: development,](#)

properties, and recycling potential of filaments. JOM 2018;70(3):303–9.
[33] Singh AK, Saltonstall B, Patil B, Hoffmann N, Doddamani M, Gupta N. Additive

manufacturing of syntactic foams: Part 2: specimen printing and mechanical property characterization. JOM 2018;70(3):310–4.

[34] Rahman AS, Mathur V, Asmatulu R. Effect of nanoclay and graphene inclusions on the low-velocity impact resistance of Kevlar-epoxy laminated composites. Compos Struct 2018;187:481–8. [35] Hassani Niaki M, Fereidoon A, Ghorbanzadeh Ahangari M. Experimental study on

the mechanical and thermal properties of basalt fiber and nanoclay reinforced polymer concrete. Compos Struct 2018;191:231–8.

[36] Wu H, Sulkis M, Driver J, Saade-Castillo A, Thompson A, Koo JH. Multi-functional ULTEM™1010 composite filaments for additive manufacturing using Fused Filament Fabrication (FFF). Addit Manuf 2018;24:298–306. [37] Weng Z, Wang J, Senthil T, Wu L. Mechanical and thermal properties of ABS/

montmorillonite nanocomposites for fused deposition modeling 3D printing. Mater Des 2016;102:276–83.

[38] Venkatesan N, Bhaskar GB, Pazhanivel K, Kesavan P. Reinforcing effect of mon- tmorillonite nanoclay on mechanical properties of high density polyethylene na- nocomposites. Appl Mech Mater 2014;591:60–3.

[39] Boran Torun S, Kiziltas A, Erbas Kiziltas E, Gardner D, Rushing T. Nanoclay re-

inforced polyethylene composites: effect of different melt compounding methods. Polym Eng Sci 2016.

[40] Rao B.N., Praveen TA, Sailaja RRN, Khan MA. HDPE nanocomposites using nanoclay, MWCNT and intumescent flame retardant characteristics. In: 2015 IEEE 11th international conference on the properties and applications of dielectric materials (ICPADM). 2015. [41] Sepet H, Tarakcioglu N, Misra RDK. Investigation of mechanical, thermal

and surface properties of nanoclay/HDPE nanocomposites produced industrially by melt mixing approach. J Compos Mater 2015;50. [42] Rotheron RN. Mineral fillers in thermoplastics: filler manufacture and characterization. Berlin, Heidelberg: Springer Berlin Heidelberg; 1999. p. 67–107. [43] Chrissafis K, Paraskevopoulos KM, Tsiaoussis I, Bikiaris D. Comparative study of the effect of different nanoparticles on the mechanical properties, permeability, and thermal degradation mechanism of HDPE. J Appl Polym Sci 2009;114(3):1606–18. [44] Alothman O. Processing and characterization of high density polyethylene/ethylene

vinyl acetate blends with different VA contents. Adv Mater Sci Eng 2012;10.

[45] Xiao K, Zhang L, Zarudi I. Mechanical and rheological properties of carbon nano-tube-reinforced polyethylene composites. Compos Sci Technol Composites Sci Technol 2007;67:177–82. [46] Bharath Kumar BR, Doddamani M, Zeltmann SE, Gupta N, Ramesh MR,

Ramakrishna S. Processing of cenosphere/HDPE syntactic foams using an industrial scale polymer injection molding machine. Mater Des 2016;92:414–23.

[47] Bharath Kumar BR, Doddamani M, Zeltmann SE, Gupta N, Uzma, Gurupadu S, Sailaja RRN. Effect of particle surface treatment and blending method on flexural properties of injection-molded cenosphere/HDPE syntactic foams. J Mater Sci 2016;51(8):3793–805.

[48] Bharath Kumar BR, Zeltmann SE, Doddamani M, Gupta N, Uzma, Gurupadu S,

Sailaja RRN. Effect of cenosphere surface treatment and blending method on the tensile properties of thermoplastic matrix syntactic foams. J Appl Polym Sci 2016;133(35).

[49] [Jayavardhan ML, Bharath Kumar BR, Doddamani M, Singh AK, Zeltmann SE, Gupta](#)

[N. Development of glass microballoon/HDPE syntactic foams by compression molding. Compos B Eng 2017;130:119–31.](#)

[50] [Jayavardhan ML, Doddamani M. Quasi-static compressive response of compression molded glass microballoon/HDPE syntactic foam. Compos B Eng 2018;149:165–77.](#) [51] [Doddamani M. Influence of microballoon wall thickness on dynamic mechanical](#)

[analysis of closed cell foams. Mater Res Express 2020;6\(12\):125348.](#)

[52] [Fouad H, Elleithy R, Al-Zahrani SM, Ali MA-H. Characterization and processing of high density polyethylene/carbon nanocomposites. Mater Des 2011;32\(4\):1974–80.](#) [53] [Yuan Q, Yang Y, Chen J, Ramuni V, Misra RDK, Bertrand KJ. The effect of crys-](#)

[tallization pressure on macromolecular structure, phase evolution, and fracture resistance of nano-calcium carbonate-reinforced high density polyethylene. Mater Sci Eng A 2010;527:6699–713.](#)

[54] [Di W, Zhang G, Xu J, Peng Y, Wang X, Xie Z. Positive-temperature-coefficient/](#)

[negative-temperature-coefficient effect of low-density polyethylene filled with a mixture of carbon black and carbonfiber. J Polym Sci B Polym Phys 2003;41\(23\):3094–101.](#)

[55] [Azeez A, Rhee KY, Park S-J, Hui D. Epoxy clay nanocomposites – processing,](#)

[properties and applications: a review. Compos B Eng 2013;45:308–20.](#)

[56] [Deka B, Maji TK. Effect of coupling agent and nanoclay on properties of HDPE, LDPE, PP, PVC blend and Phargamites karka nanocomposite. Compos Sci Technol 2010;70:1755–61.](#) [57] [Ataeefard M, Moradian S. Surface properties of polypropylene/organoclay nano-](#)

[composites. Appl Surf Sci Appl Surf Sci 2011;257:2320–6.](#)

[58] [Ataefard M, Moradian S. Polypropylene/organoclay nanocomposites: effects of clay content on properties. Polym Plast Technol Eng 2011;50:732–9.](#) [59] [Venkatesh GS, Deb A, Karmarkar A, Chauhan S. Effect of nanoclay content and compatibilizer on viscoelastic properties of montmorillonite/polypropylene nano- composites. Mater Des 2012;37:285–91.](#) [60] [Kim SG, Lofgren E, Jabarin S. Dispersion of nanoclays with poly\(ethylene ter-](#)

[ephthalate\) by melt blending and solid state polymerization. J Appl Polym Sci 2013;127.](#)

[61] [Junior J, Soares I, Luetkmeyer L, Tavares MI. Preparation of high-impact poly- styrene nanocomposites with organoclay by melt intercalation and characterization by low—field nuclear magnetic resonance. Chem Eng Process Process Intensif 2014;77.](#) [62] [Akbari B, Bagheri R. Influence of nanoclay on morphology, mechanical properties and deformation mechanism of polystyrene. Polym Plast Technol Eng 2014;53:156–61.](#) [63] [Vyas A, Iroh J. Thermal behavior and structure of clay/nylon-6 nanocomposite](#)

[synthesized by in situ solution polymerization. J Therm Anal Calorim 2014;117:39–52.](#)

[64] [Chong S, Pan G-T, Khalid M, Yang TC-K, Hung S-T, Huang C-M. Physical char- acterization and pre-assessment of recycled high-density polyethylene as 3D printing material. J Polym Environ 2016.](#) [65] [Bharath Kumar BR, Zeltmann S, Doddamani M, Gupta N, Uzma, Gurupadu S, Rrn S. Effect of cenosphere surface treatment and blending method on the tensile prop- erties of thermoplastic matrix syntactic foams. J Appl Polym Sci 2016;133.](#) [66] [Divya V, Pattanshetti V, Suresh R, Rrn S. Development and characterisation of HDPE/EPDM-g-TMEVS blends for mechanical and morphological properties for engineering applications. J Polym Res 2013;20.](#) [67] [Escocio VA, Pacheco EBAV, da Silva ALN, Cavalcante ADP, Visconte LLY. Rheological behavior of renewable polyethylene \(HDPE\) composites and sponge gourd \(Luffa cylindrica\) residue. Int J Polym Sci 2015.](#) [68] [Mohanty S, Nayak S. Short bamboo fiber-reinforced HDPE](#)

composites: influence of fiber content and modification on strength of the composite. J Reinf Plast Compos J Reinf Plast Compos 2010;29:2199–210.
[69] Shaikh H, Anis A, Poulose AM, Alam M, A-taibi MN, Alam MA, Al-Zahrani SM.

Studies on high density polyethylene reinforced with phosphate ore particles: thermal, rheological, mechanical and morphological properties. Polym Plast Technol Eng 2016;55(17):1831–41.

[70] Tanniru M, Yuan Q, Misra RDK. On significant retention of impact strength in

clay-reinforced high-density polyethylene (HDPE) nanocomposites. Polymer 2006;47(6):2133–46.

[71] Yang C, Tian X, Cao Y, Zhao F, Changquan S. Influence of thermal processing conditions in 3D printing on the crystallinity and mechanical properties of PEEK material. J Mater Process Technol 2017;248. [72] Wasiak A, Sajkiewicz P, Woźniak A. Effects of cooling rate on crystallinity of I-

polypropylene and polyethylene terephthalate crystallized in nonisothermal con- ditions. J Polym Sci B Polym Phys 1999;37(20):2821–7.

[73] Lombardi JL, Hoffinan RA, Waters JA, Popovich D. Issues associated with EFF & FDM ceramicfilled feedstock formulation. In: 1997 International Solid Freeform Fabrication Symposium. 1997. [74] Adhikary K, Park CB, Islam MR, Rizvi G. Effects of lubricant content on extrusion processing and mechanical properties of wood flour-high-density polyethylene composites. J Thermoplast Compos Mater 2011;24:155–71. [75] Ayrlimis N. Combined effects of boron and compatibilizer on dimensional stability

and mechanical properties of wood/HDPE composites. Compos B Eng 2013;44:745–9.

[76] Khalaf MN. Mechanical properties of filled high density polyethylene. J Saudi Chem Soc 2015;19(1):88–91. [77] Homaeigohar S, Sadi A,

Javadpour J, Khavandi A. The effect of reinforcement

volume fraction and particle size on the mechanical properties of β -tricalcium phosphate-high density polyethylene composites. J Eur Ceram Soc 2006;26:273–8.

[78] Sim CP, Cheang P, Liang MH, Khor KA. Injection moulding of hydroxyapatite composites. J Mater Process Technol 1997;69(1):75–8. [79] Liu H, Wu Q, Han G, Yao F, Kojima Y, Suzuki S. Compatibilizing and toughening bamboo flour-filled HDPE composites: mechanical properties and morphologies. Compos A Appl Sci Manuf 2008;39:1891–900. [80] Yuan Q, Bateman S, Wu D. Mechanical and conductive properties of carbon black-

filled high-density polyethylene, low-density polyethylene, and linear low-density polyethylene. J Thermoplast Compos Mater J Thermoplast Compos Mater 2010;23:459–71.

[81] Ou R, Xie Y, Wolcott M, Sui S, Wang Q. Morphology, mechanical properties, and

dimensional stability of wood particle/high density polyethylene composites: effect of removal of wood cell wall composition. Mater Des 2014;58:339–45.

[82] Singh R, Singh S, Fraternali F. Development of in-house composite wire based feed stock filaments of fused deposition modelling for wear-resistant materials and structures. Eng Compos B 2016;98. [83] Bharath Kumar BR, Doddamani M, Zeltmann S, Gupta N, Uzma, Gurupadu S, Rrn S. Effect of particle surface treatment and blending method on flexural properties of injection-molded cenosphere/HDPE syntactic foams. J Mater Sci

2016;51:3793–805.

[84] [Liu H, Wu Q, Zhang Q. Preparation and properties of banana fiber-reinforced composites based on high density polyethylene \(HDPE\)/Nylon-6 blends. Bioresour Technol 2009;100:6088–97.](#) [85] [Gwon JG, Lee SY, Kang H, Kim JH. Effects of sizes and contents of exothermic](#)

[foaming agent on physical properties of injection foamed wood fiber/HDPE composites. Int J Precis Eng Manuf 2012;13\(6\):1003–7.](#)

[86] [Chen HC, Chen TY, Hsu CH. Effects of wood particle size and mixing ratios of HDPE on the properties of the composites. Holz als Roh— und Werkstoff 2006;64:172–7.](#) [87] Jeyachandran Praveen, Bontha Srikanth, Bodhak Subhadip, Balla Vamsi Krishna,

Kundu Biswanath, Doddamani Mrityunjay. Mechanical behaviour of additively manufactured bioactive glass/high density polyethylene composites. J Mech Behavi Biomed Mater 2020;108.
<https://doi.org/10.1016/j.jmbbm.2020.103830>.